Available online at www.sciencedirect.com
ScienceDirect
Biochimica et Biophysica Acta 1783 (2008) 297–311
Biochimica et Biophysica Acta BBA
www.elsevier.com/locate/bbamcr

S100A8/9 induces cell death via a novel, RAGE-independent pathway that involves selective release of Smac/DIABLO and Omi/HtrA2

Saeid Ghavami [a,b], Claus Kerkhoff [c,1], Walter J. Chazin [d,e,f], Kamran Kadkhoda [a,b], Wenyan Xiao [a], Anne Zuse [a,b], Mohammad Hashemi [g], Mehdi Eshraghi [a,b], Klaus Schulze-Osthoff [h], Thomas Klonisch [i], Marek Los [a,b,i,j,k,*,1]

[a] *Manitoba Institute of Cell Biology, Canada*
[b] *Department of Biochemistry and Medical Genetics, University of Manitoba, Winnipeg, Canada*
[c] *Institute of Experimental Dermatology, Münster, Germany*
[d] *Department of Biochemistry Vanderbilt University, Nashville, TN 37232-8725, USA*
[e] *Department of Chemistry, Vanderbilt University, Nashville, TN 37232-8725, USA*
[f] *Center for Structural Biology, Vanderbilt University, Nashville, TN 37232-8725, USA*
[g] *Department of Clinical Biochemistry, School of Medicine, Zahedan University of Medical Science, Zahedan, Iran*
[h] *Institute of Molecular Medicine, University of Düsseldorf, Düsseldorf, Germany*
[i] *Department of Human Anatomy and Cell Science, University of Manitoba, Canada*
[j] *Manitoba Institute of Child's Health, University of Manitoba, Winnipeg, Canada*
[k] *BioApplications Enterprises, Winnipeg, Manitoba, Canada*

Received 4 July 2007; received in revised form 19 October 2007; accepted 23 October 2007
Available online 7 November 2007

Abstract

A complex of two S100 EF-hand calcium-binding proteins S100A8/A9 induces apoptosis in various cells, especially tumor cells. Using several cell lines, we have shown that S100A8/A9-induced cell death is not mediated by the receptor for advanced glycation endproducts (RAGE), a receptor previously demonstrated to engage S100 proteins. Investigation of cell lines either deficient in, or over-expressing components of the death signaling machinery provided insight into the S100A8/A9-mediated cell death pathway. Treatment of cells with S100A8/A9 caused a rapid decrease in the mitochondrial membrane potential ($\Delta\Psi_m$) and activated Bak, but did not cause release of apoptosis-inducing factor (AIF), endonuclease G (Endo G) or cytochrome *c*. However, both Smac/DIABLO and Omi/HtrA2 were selectively released into the cytoplasm concomitantly with a decrease in Drp1 expression, which inhibits mitochondrial fission machinery. S100A8/A9 treatment also resulted in decreased expression of the anti-apoptotic proteins Bcl2 and Bcl-X_L, whereas expression of the pro-apoptotic proteins Bax, Bad and BNIP3 was not altered. Over-expression of Bcl2 partially reversed the cytotoxicity of S100A8/A9. Together, these data indicate that S100A8/A9-induced cell death involves Bak, selective release of Smac/DIABLO and Omi/HtrA2 from mitochondria, and modulation of the balance between pro- and anti-apoptotic proteins.

Keywords: Bcl2 protein family; S100/calgranulin; Cancer regression; Drp1; Receptor for advanced glycated endproducts (RAGE); Mitochondrial fission; XIAP

Abbreviations: $\Delta\Psi_m$, mitochondrial membrane potential; AIF, apoptosis-inducing factor; BH3, Bcl2 homology 3; BNIP3, Bcl2/adenovirus E1B 19 kD-interacting protein 3; DD, death domain; DED, death effector domain; DISC, death inducing signaling complex; Drp, dynamin-related protein; DTPA, diethylene triamine pentaacetate; Endo G, endonuclease G; FADD, Fas-Associated Death Domain; FADD-DN, dominant-negative FADD mutant; HtrA2, high-temperature requirement A2; IAPs, inhibitors of apoptosis; IM, inner membrane; JC-1, 5,5′,6,6′-tetrachloro-1,1′,3,3′-tetraethylbenzimidazolylcarbocyanine iodide; MTT, 3-(4,5-dimethyl-2-thiazolyl)-2,5-diphenyl-2H-tetrazolium bromide; RAGE, receptor for advanced glycation endproducts; ROS, reactive oxygen species; Smac/DIABLO, second mitochondrial activator of caspases/direct inhibitor of apoptosis binding protein of low PI; XIAP, X-linked inhibitor of apoptosis

* Corresponding author. BioApplications Enterprises, Canada. Tel.: +1 204 334 5192.
E-mail address: mjelos@gmail.com (M. Los).
[1] Both authors share senior authorship.

0167-4889/$ - see front matter © 2007 Elsevier B.V. All rights reserved.
doi:10.1016/j.bbamcr.2007.10.015

1. Introduction

Polymorphonuclear neutrophils, a vital component of the innate immune response, perform several host-defense functions such as phagocytosis of invading microorganisms and cell debris, release of a number of arachidonic acid-derived eicosanoids, generation of reactive oxygen species (ROS), and release of proteolytic enzymes as well as bactericidal and cytotoxic peptides. A complex, of two S100 EF-hand proteins, S100A8/A9, is one component of this system. S100A8/A9 is released from activated phagocytes and exerts antimicrobial activity as well as cytotoxicity against various tumour cells [1–3].

S100A8 and S100A9 (also known as calgranulins A and B, or MRP8 and MRP14 respectively) are members of the S100 multigene subfamily of cytoplasmic EF-hand Ca^{2+}-binding proteins [4,5]. They are differentially expressed in a wide variety of cell types and are abundant in myeloid cells. High expression of S100A8 and S100A9 has been reported in disorders such as rheumatoid arthritis, inflammatory bowel disease and vasculitis [5]. The S100A8/S100A9 complex is located in the cytosol of resting phagocytes and exhibits two independent translocation pathways when the cells are activated. Therefore, it has been assumed that membrane-associated and soluble S100A8/A9 may have distinct cellular functions. Recent data suggest that intracellular S100A8/A9 might be involved in (phagocyte) NADPH oxidase activation [6], whereas the secreted form exerts antimicrobial properties and induces apoptosis [1–3].

S100 proteins are known to bind to RAGE, and this interaction is considered to represent a novel proinflammatory axis involved in several inflammatory diseases. S100 activation offers an attractive model to explain how RAGE and its pro-inflammatory ligands might contribute to the pathophysiology of such diseases (for review see [7,8]). RAGE is expressed in many cell types, including endothelial cells, smooth muscle cells, lymphocytes, monocytes and neurons. RAGE comprises an extracellular region containing three immunoglobulin-like domains followed by a transmembrane domain and a short cytoplasmic region. Although intracellular binding partners have not yet been identified, the cytoplasmic region appears to be essential for RAGE signaling (for review see [9]). Binding of ligands to RAGE contributes not only to perturbation of cell homeostasis under pathological conditions [7], but also to cell migration and differentiation [10]. Evidence has accumulated that S100A8/A9 induces cell death through a dual mechanism: one associated with zinc extraction from the target cells, the other through binding to the target cell surface, possibly via ligand-induced receptor activation [1]. While the zinc-chelating activities have been characterized [11,12], the S100A8/A9 cell surface receptor and the signaling pathway have not been identified.

In the present study we provide new, important insight into the molecular mechanisms of S100A8/A9-induced cell death. Our data shows that S100A8/A9-triggered cell death, does not involve RAGE, or FADD-dependent death receptors, but is mediated by selected components of the mitochondrial death pathway. We have demonstrated that S100A8/A9-induced cell death is modulated by Bcl2-family members, and also relies on mitochondrial release of OMI/HtrA2 and Smac/DIABLO, but not cytochrome *c*, AIF, or Endo G. These events are concomitant with XIAP cleavage and downregulation of Drp1, that regulates mitochondrial fission.

2. Materials and methods

2.1. Materials

Cell culture media were purchased from Sigma Co. (Canada, Oakville, ON) and Gibco (Canada). Cell culture plasticware was obtained from Nunc Co. (Canada). Diethylene triamine pentaacetate (DTPA) and 3-(4,5-dimethyl-2-thiazolyl)-2,5-diphenyl-2H-tetrazolium bromide (MTT), monoclonal antibody to human MRP8/14 (FITC-labeled, clone 27 E10, Acris, Germany), rabbit anti-human Bak, mouse anti-human Bax, mouse anti-human Bcl-X_L, rabbit anti-human Mcl-1, and mouse anti-human BNIP3 were obtained from Sigma (Sigma-Aldrich, Oakville, CA), rabbit anti-human/mouse Bcl2, rabbit anti-human/mouse/rat Drp1, anti-human/mouse/rat glyceraldehyde-3-phosphate dehydrogenase (GAPDH), rabbit anti-human/mouse/rat Smac/DIABLO, rabbit anti-human/mouse/rat Omi/HtrA2, mouse anti-human/mouse/rat cytochrome *c*, and goat anti-human/mouse/rat endonuclease G (Endo G) were obtained from Santa Cruz Biotechnologies (USA). 5,5′,6,6′-tetrachloro-1,1′,3,3′-tetraethyl-benzimidazolylcarbocyanine iodide (JC-1) was obtained from Invitrogen Molecular Probes (Canada). Human RAGE-siRNA and siRNA negative control were obtained from Santa Cruz Biotechnologies (USA). Goat anti-human RAGE blocking antibody was obtained form R&D Systems (Hornby, ON, CA). Anti-CD95 IgM was obtained from Upstate Cell Signaling (CA).

2.2. Purification of S100A8 and S100A9 from human neutrophils

Human neutrophils were prepared from leukocyte-rich blood fractions ("buffy coat"). S100A8/A9 was purified as described earlier [13]. Prior to use, the proteins were re-chromatographed by anion exchange using a UnoQ column (BioRad, Munich, Germany). Recombinant protein was produced by bacterial over-expression as previously described [14]. All experiments were performed using S100A8/A9 purified from human neutrophils and the results were confirmed using recombinant S100A8/A9 [14].

2.3. Cell culture

MCF7 (human, estrogen receptor positive breast cancer), MCF7-Bcl2 over-expressing, MDA-MB231 (human, estrogen receptor negative breast cancer), Jurkat (human T-cell leukemia), Jurkat-Bcl2 over-expressing, Jurkat FADD-DN, BJAB (murine B cell leukemia), BJAB FADD-DN, L929 (murine fibrosarcoma), HEK-293 (human embryonic kidney), and SHEP and KELLY (human neuroblastomas) were cultured in RPMI-1640 or DMEM (MDA-MB231, L929, HEK-293) supplemented with 10% fetal calf serum, 100 U/ml penicillin and 100 μg/ml streptomycin. Cells were incubated at 37 °C in a humidified atmosphere of 5% CO_2. Cell cultures were maintained under logarithmic growth conditions.

2.4. MTT-assay

The cytotoxicity of S100A8/A9 and DTPA towards the above indicated cell lines was determined by MTT-assay as previously described [15,16]. Cell viability was calculated as a percentage using the equation: (mean OD of treated cells/mean OD of control cells) × 100 (for each time point the treated cells were compared with control cells which were treated only with solvent of S100A8/A9 and DTPA).

2.5. Measurement of apoptosis by flow cytometry

Apoptosis was measured using the Nicoletti method [17]. Briefly, cells grown in 12-well plates were treated with S100A8/A9 (100 μg/ml) for the indicated time intervals. After scraping, the cells were harvested by centrifugation at 800 g for

5 min, washed once with PBS, and then resuspended in a hypotonic propidium iodide (PI) lysis buffer (1% sodium citrate, 0.1% Triton X-100, 0.5 mg/ml RNase A, 40 μg/ml propidium iodide). The cell nuclei were then incubated for 30 min at 30 °C and subsequently analyzed by flow cytometry. Nuclei to the left of the G1 peak containing hypodiploid DNA were considered to be apoptotic.

2.6. Determination of specific S100A8/A9 binding sites on the cell surface

Harvested cells were washed three times with PBS containing 3% bovine serum albumin (BSA) and 0.05% sodium azide (NaN_3) (B-PBS). A total of 2×10^6 cells were incubated with 10 μg of human S100A8/A9 for 1 h, washed three times with B-PBS, and then incubated for 30 min in absence of light with 200 μl FITC-labeled anti-S100A8/A9 antibody (1:50) (murine IgG1 clone 27E10) containing 20 μg/ml propidium iodide in order to gate out dead cells. Finally, they were washed three times with B-PBS. In order to control for non-specific binding of the FITC-labeled anti-S100A8/A9, the cells were incubated with FITC-labeled antibody in the absence of human S100A8/A9 [18]. The stained cells were analyzed by flow cytometry (FACS-Calibur, Cell Quest Pro software).

2.7. Immunoblotting

The expression of RAGE, XIAP, Bcl2, Bcl-X_L, Mcl-1, Bax, Bak and BNIP3 in SHEP cells, that had been treated with 100 μg/ml S100A8/A9 for different time intervals was determined by Western blotting. In order to prepare cell lysates, treated cells were harvested, washed once with cold PBS and resuspended for 20 min on ice in a lysis buffer: 20 mM Tris–HCl (pH 7.5), 0.5% Nonidet P-40, 0.5 mM PMSF and 0.5% protease inhibitor cocktail (Sigma). The lysate was centrifuged at 10,000 g and the supernatant was collected. 30 μg of total protein was separated by SDS-PAGE and then transferred onto nylon membranes (Bak dimerization was detected in non-reducing conditions). The membranes were blocked in 5% non-fat dried milk in Tris-buffered saline–Tween 0.1% (TBS) (0.05 M Trizma base, 0.9% sodium chloride and 0.1% Tween-20), then incubated overnight with the primary antibodies at 4 °C. The membranes were then incubated at room temperature for 1 h with the relevant secondary antibodies conjugated with HRP, and membranes were developed by enhanced chemiluminescence (ECL) detection (Amersham-Pharmacia Biotech).

2.8. RNA interference (RNAi)

The target siRNA for RAGE (sc-36374) and a negative control siRNA (sc-37007) with an irrelevant sequence were purchased from Santa Cruz Biotechnologies. The cells were grown to 60–80% confluence and then transfected with the siRNA duplex (final concentration 100 nM) using Lipofectamine (Invitrogen) according to the manufacturer's instructions. RAGE expression was determined by immunoblotting at 0, 24, 48 and 72 h post-transfection. The transfected cells (72 h post-transfection) were then treated with 0–80 μg/ml S100A8/A9 for 48 h and the viability was assessed by MTT-assay.

2.9. Blocking of RAGE with specific blocking antibody

Cells were grown in 96-well plates. After 24 h, they were treated with RAGE blocking antibody (166 μg/ml) for 1 h, then treated with S100A8/A9 (0–80 μg/ml) for another 48 h. Viability was assessed using MTT-assay.

2.10. Mitochondrial membrane potential

The assay was performed using a mitochondria-specific cationic dye (JC-1), which undergoes membrane potential-dependent accumulation in the mitochondria. JC-1 exists as a monomer when the membrane potential ($\Delta\Psi_m$) is lower than 140 mV and emits green light (540 nm) after excitation by blue light (490 nM) [19]. At higher membrane potentials, JC-1 monomers are converted to aggregates that emit red light (590 nm) after excitation by green light (540 nm). MCF7 and MCF7 Bcl2 over-expressing cells were seeded in black clear-bottom 96-well plates. Following treatment with 100 μg/ml S100A8/A9 for different time intervals as indicated, the cells were loaded with JC-1 by replacing the culture medium with HEPES buffer (40 mM, pH 7.4) containing 4.5 g/l glucose (high glucose medium) or 1.5 g/l glucose (low glucose medium), 0.65% NaCl and 2.5 μM JC-1 for 30 min at 37 °C, then washed once with HEPES buffer. Fluorescence was measured after a further 90 min (this time period is sufficient for JC-1 to equilibrate between the cytosol and mitochondrial compartments as ascertained in preliminary experiments) using a fluorescence plate reader that allows for the sequential measurement of each well at 2 excitation/emission wavelength pairs, 490/540 and 540/590 nm. Changes in the ratio between the measured red (590 nm) and green (540 nm) fluorescence intensities indicate changes in mitochondrial membrane potential. This ratio was calculated for each well after the fluorescence intensity of wells containing medium and serum without cells was subtracted. The ratio of red to green fluorescence in the same culture depends only on the membrane potential and is independent of other factors such as cell number and mitochondrial size, shape and density.

2.11. Cell fractionation

Cytoplasmic and mitochondrial fractions were separated by differential centrifugation [17,20]. Briefly, the cells were treated S100A8/A9 (100 μg/ml), then harvested and washed once with PBS after the indicated time points. Cells were resuspended for 5 min on ice in a lysis buffer: 10 mM Tris–HCl (pH 7.8), 1% Nonidet P-40, 10 mM mercaptoethanol, 0.5 mM PMSF, 1 mg/ml aprotinin and 1 mg/ml leupeptin. An equal amount of distilled water was added to the cells to enhance lysis. The cells were then sheared by passing them through a 22-gauge needle. The nuclear fraction was recovered by centrifugation at 600 g for 5 min, and the 'low-speed' supernatant was centrifuged at 10,000 g for 30 min to obtain the mitochondrial (pellet) and cytosolic (supernatant) fractions. The mitochondrial fraction was further lysed in 10 mM Tris (pH 7.4), 150 mM NaCl, 1% Triton X-100, and 5 mM EDTA (pH 8.0).

2.12. Immunocytochemistry, confocal imaging and electron microscopy

Cells were grown overnight on coverslips and then treated with 100 μg/ml S100A8/A9. After 12 h, they were washed with PBS and fixed in 4% paraformaldehyde, then permeabilized with 0.1% Triton X-100. To locate cytochrome *c*, Smac/DIABLO, AIF, and Endo G, the cells were incubated with anti-cytochrome *c* mouse IgG (1:100 dilution), anti-Smac rabbit IgG (1:100 dilution), anti-DIABLO rabbit IgG (1:150 dilution), anti-Endo G goat IgG (1:75 dilution), anti-AIF mouse IgG (1:500 dilution), respectively. After three washes with PBS, the cytochrome *c*, AIF-antibody complexes were stained with the corresponding Cy5-conjugated secondary antibodies (Sigma, 1:1500 dilution), and Endo G, Smac and DIABLO were stained with the corresponding FITC-conjugated secondary antibodies (Sigma, 1:40 dilution) then washed three times with PBS. To visualize nuclei, cells were stained with 10 μg/ml DAPI. The mitochondria were stained with the mitochondria-specific dye Mitotracker Red CMXRos (Molecular Probes; 200 nM in RPMI medium) for 15 min prior to fixing. The fluorescent images were then observed and analyzed using an Olympus-FV500 multi-laser confocal microscope.

For transmission electron microscopy, cells were fixed in 2.5% glutaraldehyde in PBS (pH 7.4) for 1 h at 4 °C, washed and fixed in 1% osmium tetroxide, before embedding in Epon. Transmission electron microscopy was performed with a Philips CM10, at 80 kV, on ultra-thin sections (100 nm on 200 mesh grids) stained with uranyl acetate and counterstained with lead citrate.

2.13. Statistical analysis

The results were expressed as means ± SD and statistical differences were evaluated by one-way and two-way ANOVA followed by Tukey's post-hoc test, using the software package SPSS 11. $P < 0.05$ was considered significant.

3. Results

3.1. S100A8/A9 kills cancer cells of various histological origins by apoptosis

The apoptosis-inducing activity of S100A8/A9 was investigated in the cell lines MCF7, MDA-MB231, Jurkat, BJAB,

HEK-293, L929, SHEP and KELLY. MTT was used to determine the cytotoxic activity of S100A8/A9 (Supplementary Fig. 1A). To control for the zinc ion-depleting effect of S100A8/A9, we performed experiments with the membrane-impermeable Zn^{+2} chelator DTPA (Supplementary Fig. 1B). Experiments were repeated using the Nicoletti method, a flow cytometry technique that detects hypodiploid nuclei typical of apoptosis, to confirm that cell death was occurring via apoptosis (data not shown). In a parallel experiment, caspase activation and PARP-1 cleavage were investigated using SHEP cells, which were treated with S100A8/A9 (100 μg/ml) for 24 h. Our results showed significant increase in caspase-3, -9, -6, and -7 and PARP-1 cleavage in treated cells (data not shown).

The tested cell lines showed remarkable differences in sensitivity with respect to time course and effective dose. S100A8/A9 at 100 μg/ml induced significant cell death ($P<0.05$) in all cell lines tested, but a 50% drop in cell viability was determined at different time intervals for the individual lines (Supplementary Fig. 1A). The EC_{50} of S100A8/A9 after 48 h of treatment were as follows: MDA-MB231 EC_{50}= 45 μg/ml, SHEP EC_{50}=85 μg/ml, KELLY EC_{50}=110 μg/ml, and BJAB EC_{50}=35 μg/ml. In contrast, DTPA did not induce significant cell death in MDA-231, L929, and HEK-293 cells (Supplementary Fig 1B). We have previously shown that DTPA cytotoxicity was completely inhibited by Zn^{+2} co-treatment, while the apoptosis-inducing activity of S100A8/A9 is only partially reversed by the addition of zinc [1]. These data confirmed that the apoptosis-inducing activity of S100A8/A9 is not entirely dependent on zinc depletion.

3.2. RAGE is not involved in cell death signaling by S100A8/A9

Experiments were performed to analyze the specific binding of S100A8/A9 to certain cell lines and the corresponding levels of RAGE expression. The indicated cell lines were incubated in the presence and absence of S100A8/A9, and the amount bound to the cells was measured by flow cytometry using the FITC-labeled monoclonal antibody 27E10, which specifically recognizes the S100A8/A9 heterodimer. The fluorescence in the absence of S100A8/A9 (non-specific binding) was subtracted from the fluorescence determined in its presence. The data were analyzed using CellQuest Pro software. All the cell lines investigated expressed S100A8/A9-specific binding sites (Fig. 1A). Subsequently, RAGE expression in these cells was confirmed by Western blotting. As shown in Fig. 1B, RAGE-specific immunoreactivity was detected in all cell lines.

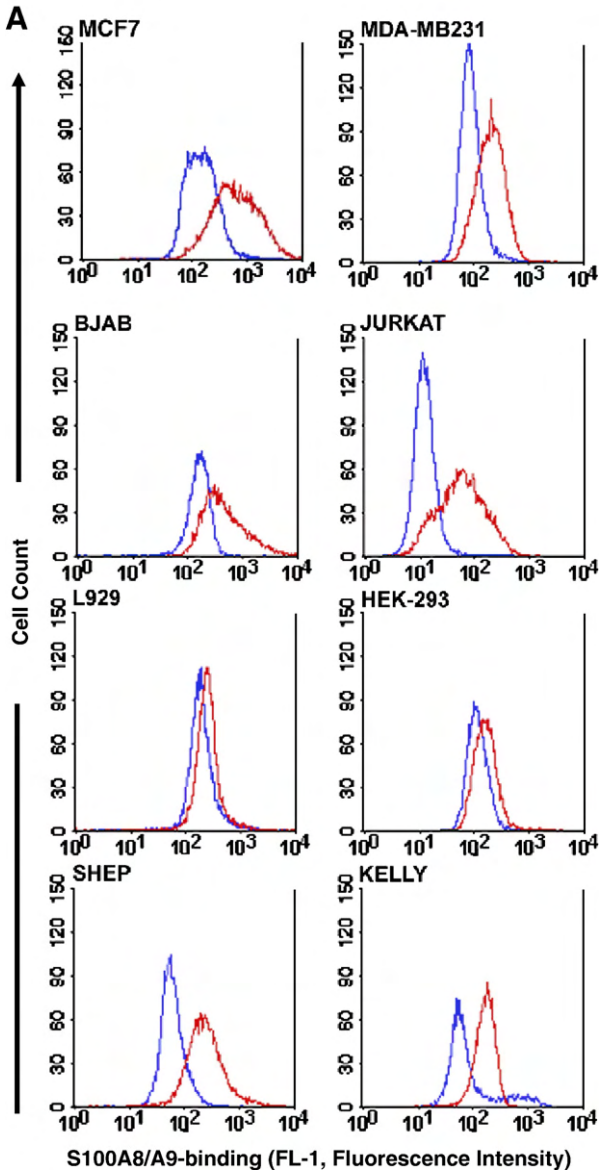

Fig. 1. Induction of apoptosis by S100A8/A9 does not depend on its interaction with RAGE. (A) Binding of S100A8/A9 to various cell lines as detected by flow cytometry. Cells (2×10^6) were incubated with PBS supplemented with 3% BSA (B-PBS) and 10 μg/ml S100A8/A9 on ice for 1 h, and washed three times with cold B-PBS. They were then incubated with FITC-labeled anti-S100A8/A9 for 30 min on ice, and were finally washed three times with cold B-PBS. The FITC-signal was detected in the FL-1 channel by flow cytometry. The blue histogram shows non-specific binding and the red shows total signal. Non-specific binding is the binding of FITC-labeled anti-S100A8/A9 in absence of S100A8/A9. (B) RAGE expression in various cell lines, detected by Western blot (see the Materials and methods section for more details). (C) Inhibition of RAGE expression by specific siRNA, in MDA-MB231 cells. The changes in RAGE expression, were monitored by Western blot. Scrambled siRNA was used as a negative control. Cellular proteins were extracted at 0, 24, 48, and 72 h post-transfection. GAPDH was used as a loading control. (D) Specific binding of S100A8/A9 to MDA-MB231 (blue), negative control siRNA transfected MDA-MB231 cells (green), and RAGE-targeting siRNA transfected cells (red). Cells were harvested 72 h post-transfection and S100A8/A9 binding was monitored by flow cytometry. The data shows that RAGE-siRNA partially decreased S100A8/A9 binding to MDA-MB231. (E) Cytotoxicity of S100A8/A9 on MDA-MB231 cells transfected with RAGE-targeting siRNA or negative control siRNA. For each time point the treated cells were compared with control cells, which were treated with culture medium and S100A8/A9 solvent (PBS). Cell viability was assessed by MTT-assay. Results are expressed as percentage deviation from control and represent means±SD of four independent experiments. (F–H) Cytotoxicity of S100A8/A9 on MDA-MB231 (F), HEK-293 (G), and SHEP cells (H) in the presence of RAGE blocking antibody (166 μg/ml). Cell viability was assessed by MTT-assay. For each time point the treated cells were compared with control cells treated with S100A8/A9 solvent (PBS). Results are expressed as percentage deviation from control and represent means±SD of four independent experiments.

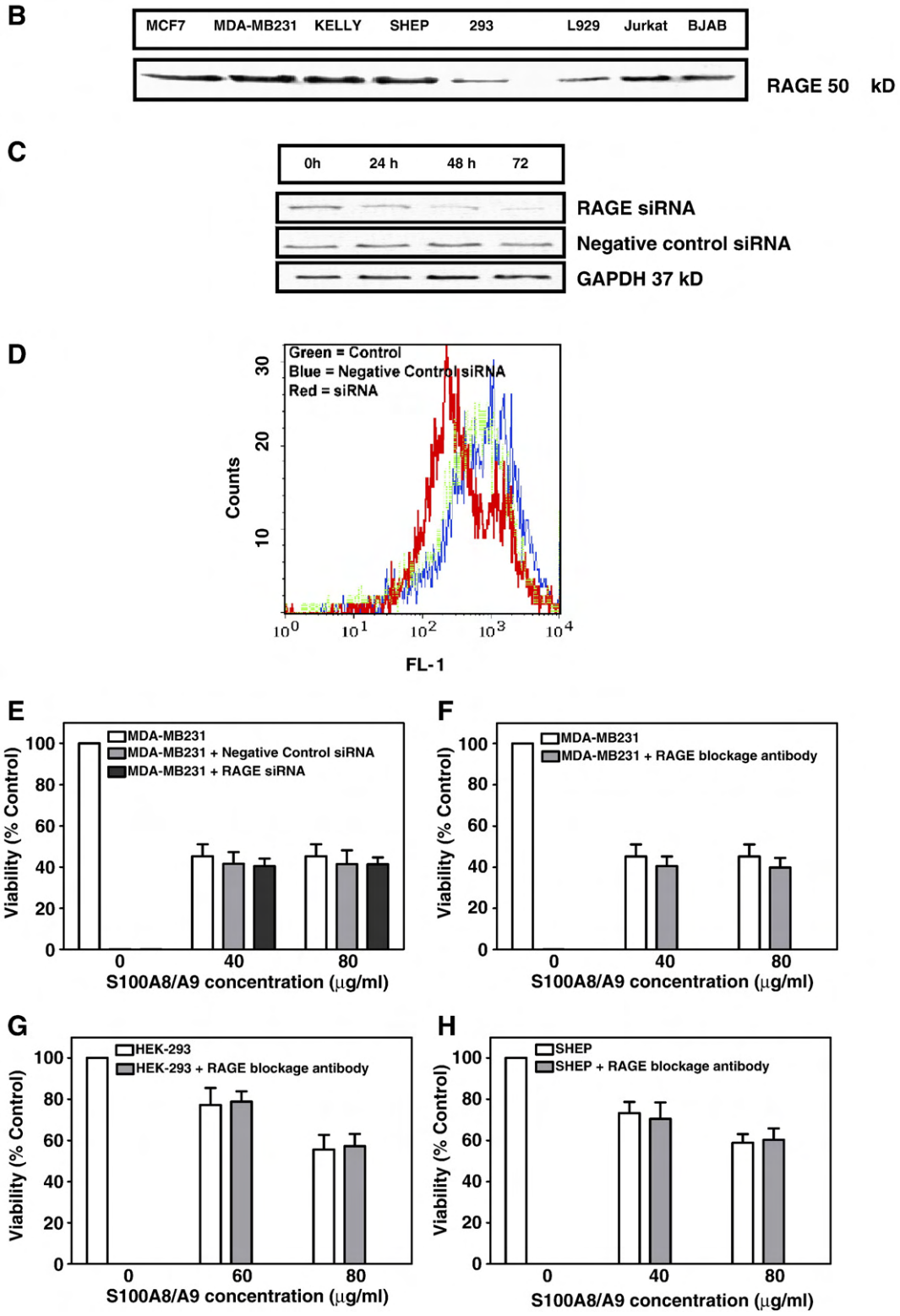

Fig. 1 (*continued*).

To explore whether ligand-induced RAGE activation was responsible for S100A8/A9's cytotoxicity, RAGE expression in MDA-MB231 (Fig. 1C), SHEP, and HEK-293 cells (data not shown) was inhibited by the specific siRNA. The expression decreased with increasing incubation time, and after 72 h, RAGE protein was nearly undetectable. The specific siRNA almost completely down-regulated RAGE expression, whereas the negative control siRNA had no effect. S100A8/A9 binding to MDA-MB231 cells treated for 72 h with either RAGE-specific siRNA or negative control siRNA was measured by

flow cytometry (Fig. 1D). Blocking of RAGE expression by the specific siRNA resulted in significantly lower binding of S100A8/A9 than in either the untreated or the negative control siRNA-treated cells, indicating that S100A8/A9 binds to RAGE.

We next investigated the induction of apoptosis by S100A8/A9 in MDA-MB231 cells that were treated either with the specific siRNA to suppress RAGE expression or with the negative control siRNA. As shown in Fig. 1E, S100A8/A9-induced cell death levels were similar in both cell populations. Furthermore, we performed viability assays on MDA-MB231, SHEP and HEK-293 cells in the presence of S100A8/A9 and a RAGE-specific blocking antibody (Fig. 1F–H). This experiment confirmed that blocking of RAGE did not prevent S100A8/A9 from inducing apoptosis. These data confirm that although RAGE is a receptor for S100A8/A9, RAGE-mediated signaling is not involved in S100A8/A9-mediated cytotoxicity. Thus, either another receptor is responsible for S100A8/A9-mediated pro-apoptotic activity, or S100A8/A9 induces apoptosis by a so far undiscovered receptor-independent mechanism.

3.3. S100A8/A9-induced cell death is not dependent on a cell death pathway involving FADD

In order to gain insight into the S100A8/A9 death signaling pathway, we investigated the apoptosis-inducing activity of S100A8/A9 in Jurkat and BJAB cells over-expressing FADD-DN, which prevents the formation of a functional DISC. Activation of caspase-8 in these experiments is triggered not only by CD95-L/Fas-L, but also by TRAIL or activating anti-APO-1 antibodies [21]. We treated the two cell lines and their wild type controls with 100 μg/ml S100A8/A9 for the indicated time (Fig. 2A,B). The FADD-DN over-expressing cells did not differ from the corresponding wild type cells in their sensitivity towards S100A8/A9. In a control experiment, wild type Jurkat cells and Jurkat over-expressing FADD-DN were treated with an agonistic anti-CD95 antibody (Fig. 2C). While wild type Jurkat cells showed increased cell death with increasing anti-CD95 concentrations, the Jurkat-FADD-DN cells remained resistant. These results are in accord with our previous study demonstrating that S100A8/A9 did not induce caspase-8 activation in HT29/219 and SW742 cells [1].

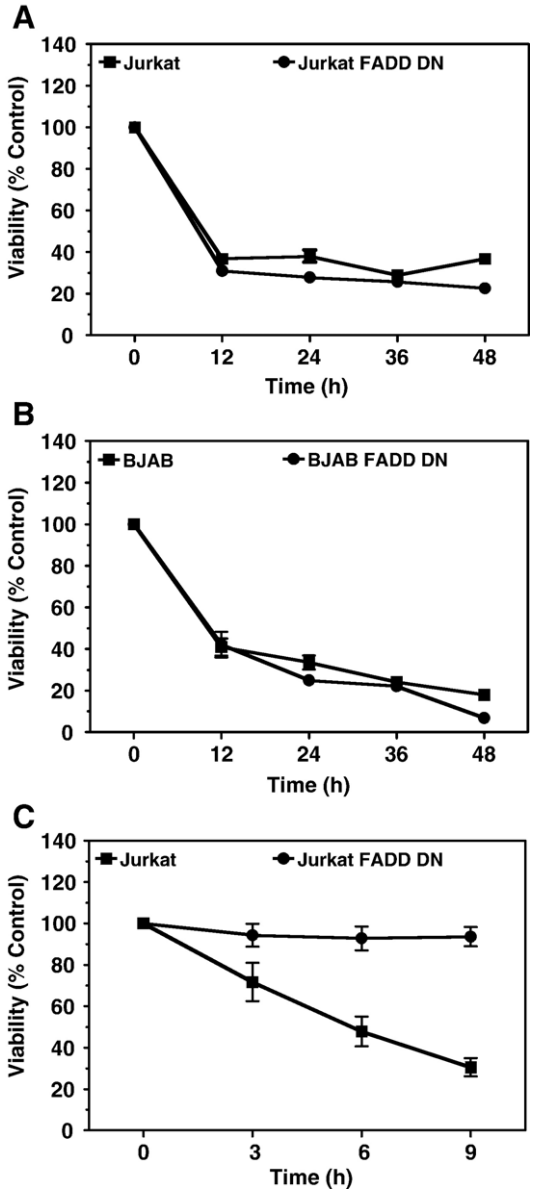

Fig. 2. Apoptosis induction by S100A8/A9 is not mediated by FADD-dependent death receptor pathways. (A,B) Cytotoxicity of S100A8/A9 (100 μg/ml) on (A) Jurkat or (B) BJAB cells over-expressing FADD-DN. (C) Control experiment: apoptosis-inducing activity of anti-CD95 antibody (500 ng/ml) on Jurkat, or Jurkat cells over-expressing FADD-DN. Cell viability was assessed by MTT-assay. For each time point the treated cells were compared with control cells treated with S100A8/A9 solvent (PBS). For control of anti-CD95 antibody the cells were treated with volume of PBS, equal to anti-CD95-antibody. Results are expressed as percentage of corresponding control and represent the means± SD of four independent experiments.

3.4. Over-expression of Bcl2 partially blocks S100A8/A9-induced apoptosis

Previous studies have shown that S100A8/A9 causes the production of reactive oxygen species and that S100A8/A9-induced cell death is inhibited by *N*-acetyl-cysteine [1,22]. Hence, we investigated the involvement of mitochondria in S100A8/A9-induced cell death. Over-expression of Bcl2 has been shown to block apoptosis that involves the mitochondrial death pathway [23]. We therefore investigated the induction of apoptosis by S100A8/A9 in two cell lines over-expressing Bcl2 and the corresponding wild type counterparts. Both Bcl2-over-expressing cell lines, Jurkat-Bcl2 and MCF7-Bcl2, were significantly more resistant to S100A8/A9 than the wild type controls (Fig. 3A,B). Bcl2-over-expression was not sufficient to block S100A8/A9-triggered cell death completely. Since Bcl2 over-expression conferred resistance to the apoptosis-inducing activity of S100A8/A9, we investigated the loss of mitochondrial membrane potential ($\Delta\Psi_m$) using JC-1 in these Bcl2 over-expressing cell lines (Fig. 3C). S100A8/A9 caused a rapid decrease of $\Delta\Psi_m$ in wild type MCF7, while MCF7 cells over-expressing Bcl2 showed a less pronounced decrease mitochondrial depolarization (Fig. 3C).

3.5. S100A8/A9 decreases the expression of the anti-apoptotic proteins Bcl2 and Bcl-X_L

Bcl2 and Bcl-X_L are two anti-apoptotic members of the large Bcl2 family of proteins. The protective, anti-cell death effect of Bcl2 is counteracted by Bax and other pro-apoptotic Bcl2-family members, which heterodimerize with anti-apoptotic Bcl2 proteins. The balance between pro- and anti-apoptotic proteins determines the fate of the cell [24]. In addition, it was recently reported that expression of anti-apoptotic Bcl2 family members played an important role in the preservation of Ψ_m [25]. Because the balance between anti-apoptotic and pro-apoptotic members of the Bcl2-family of proteins is important, we investigated if changes in expression of certain members of this family occurred in SHEP cells treated with S100A8/A9. Similar results were obtained in experiments using MCF7 cells (data not shown). As shown in Fig. 3, S100A8/A9 treatment caused a decrease in Bcl2 and Bcl-X_L levels. The expression of Mcl-1, Bax, BNIP3 and Bak was not altered (Fig. 3D). These data indicate that S100A8/A9 affects Bcl2 and Bcl-X_L expression, thereby increasing the ratio of pro- to anti-apoptotic proteins and facilitating cell death.

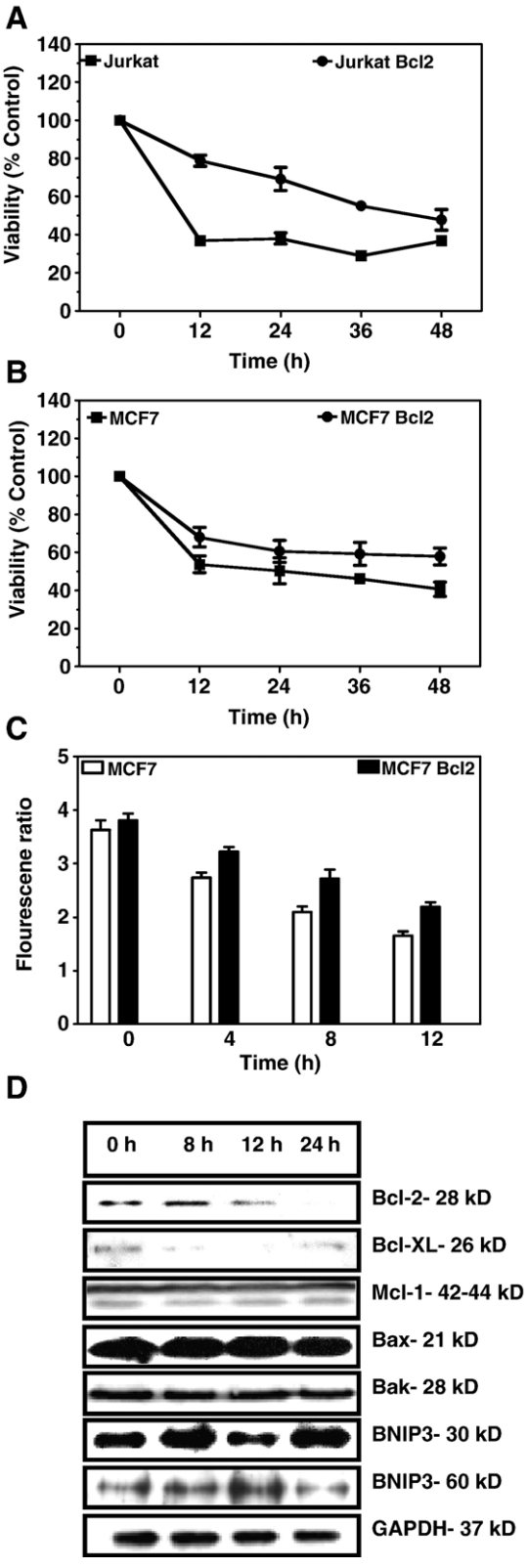

Fig. 3. The effect of Bcl2 on S100A8/A9-mediated cytotoxicity. Jurkat cells over-expressing Bcl2 (A), MCF7 cells over-expressing Bcl2 (B), and the corresponding wild type cells were treated with S100A8/A9 (100 μg/ml) for the indicated time. For each time point the treated cells were compared to control cells, treated with S100A8/A9 solvent (PBS). Cell viability was assessed by MTT-assay. Results are expressed as percentage of corresponding control and represent the means ± SD of four repeats. (C) Bcl2 over-expression decreases the loss of mitochondrial membrane potential ($\Delta\Psi_m$) after treatment with S100A8/A9 (100 μg/ml). MCF7, and MCF7 over-expressing Bcl2, were treated with S100A8/A9 and $\Delta\Psi_m$ was determined by flow cytometry, using JC-1 fluorescent dye. (D) S100A8/A9 treatment lowered the expression of anti-apoptotic proteins Bcl2 and Bcl-X_L. Western blot analysis of Bcl2, Bcl-X_L, Mcl-1, Bax, Bak, and BNIP3 expression in SHEP cell lysates treated with 100 μg/ml S100A8/A9 for 0, 8, 16 and 24 h. GAPDH was included as loading control.

3.6. S100A8/A9 triggers selective release of Smac/DIABLO and Omi/HtrA2, and downregulates DRP1 expression

To further examine the effect of S100A8/A9 on mitochondria, we monitored the release of various factors known to play a role in the mitochondrial death pathway. During the apoptotic process, the mitochondrial outer and inner membranes are both permeabilized resulting in the release of soluble proteins from the organelle. These include the mitochondrial FAD-dependent oxidoreductase AIF [26], the mitochondrial nuclease Endo G [27], and caspase activators: cytochrome *c*, Smac/DIABLO and Omi/HtrA2 (for review see [28]).

We therefore treated SHEP, MCF7 and L929 cells with 100 μg/ml S100A8/A9 for 12 h and examined the subcellular locations of cytochrome *c*, Smac/DIABLO, Omi/HtrA2, Endo G and AIF by confocal imaging (Fig. 4A–E). Cytochrome *c*, Smac/DIABLO, Omi/HtrA2, AIF and Endo G immunofluorescence signals were present in the mitochondria of untreated cells (Fig. 4A–E, control panel). In contrast, no translocation of AIF (Fig. 4D, S100A8/A9 panel) or Endo G (Fig. 4E, S100A8/A9 panel) to the nucleus, or release of cytochrome *c* (Fig. 4A, S100A8/A9 panel) from mitochondria, was observed after S100A8/A9 treatment. These results indicate that the release of AIF, Endo G, and cytochrome *c* is not involved in S100A8/A9-dependent cell death. Interestingly, Smac/DIABLO and Omi/HtrA2 were released selectively from the mitochondria to the

cytosol in S100A8/A9-treated cells (Fig. 4B,C), indicating that these proteins are involved in S100A8/A9-induced cell death. Similar observations were made for MCF7 and L929 cells (data not shown). Translocation of Smac/DIABLO and Omi/HtrA2 was also confirmed by immunoblotting of the cytosolic and mitochondrial fractions of S100A8/A9-treated cells (Fig. 4H,I). Translocation of cytochrome *c*, Endo G, and AIF was also investigated with immunoblotting of cytosolic, nuclear and mitochondrial fractions (data not shown).

The release of cytochrome *c*, Smac/DIABLO, Omi/HtrA2, AIF and Endo G during apoptosis is known to be regulated by a subclass of Bcl2 proteins [29–31], including Bax and Bak. These proteins are in an inactive state in healthy cells, with Bax predominantly found in the cytosol. However, upon the onset of apoptosis induced by various death stimuli, including DNA damage and trophic factor deprivation, they are activated by a process requiring BH3-only Bcl2 family members [30]. SHEP, MCF7 and L929 cells were therefore treated with 100 μg/ml

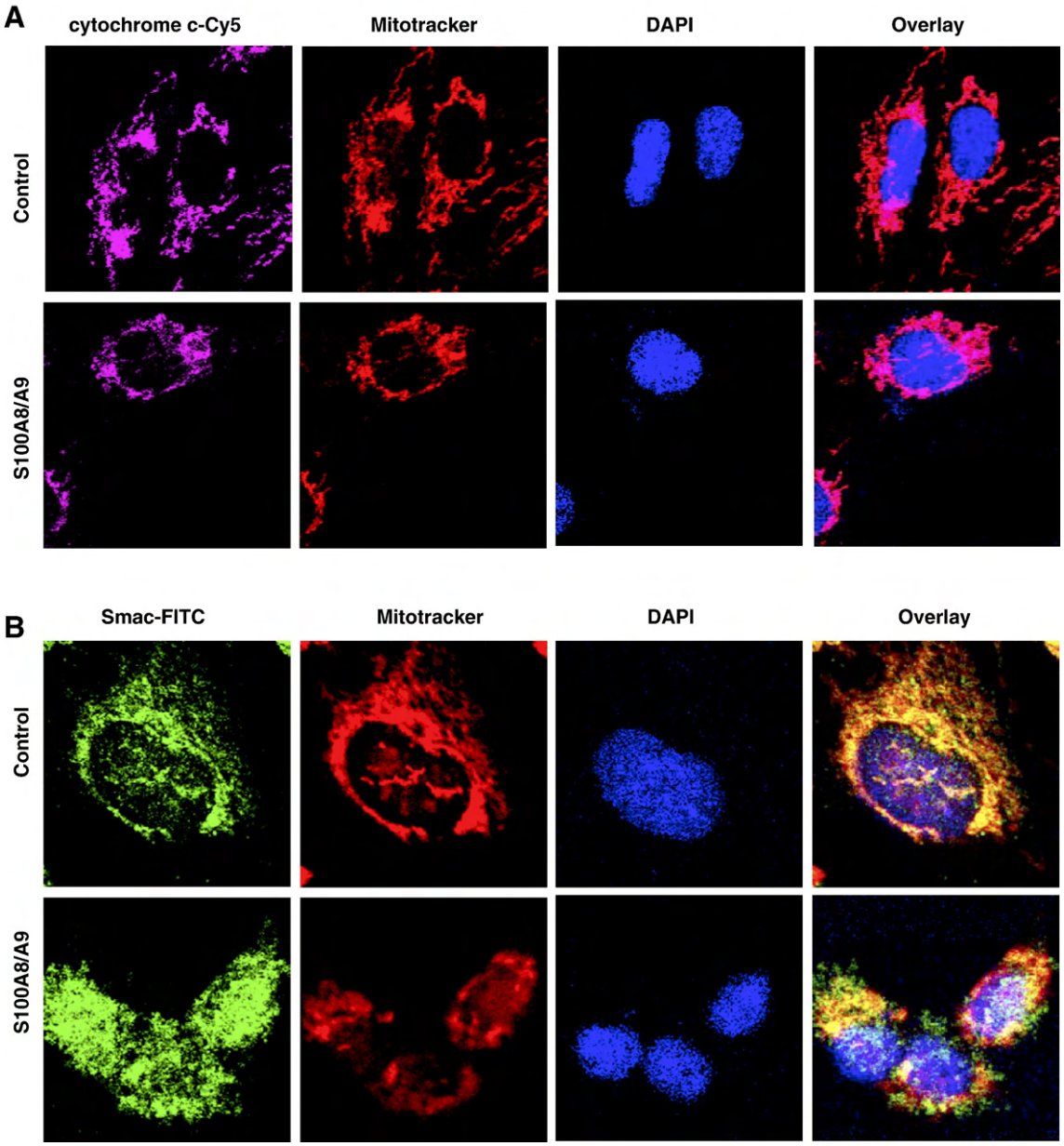

Fig. 4. The involvement of mitochondrial pro-apoptotic proteins in S100A8/A9-triggered cell death. Cellular localization of cytochrome *c* (A), Smac/DIABLO (B), Omi/HtrA2 (C), AIF (D), endonuclease G (E), and Bax (F) in SHEP cells by confocal microscopy. Cells were treated with 100 μg/ml S100A8/A9 for 12 h, see the Materials and methods section for further details. Western blot analysis of Bak (G), Smac (H), Omi (I), and DRP1 (J) in S100A8/A9-treated cells. Western blot detection was performed as described in the Materials and methods section. GAPDH was used as loading control. Cellular localization of Smac/DIABLO (K,L) mitochondrial ultrastructure in control (K) and SHEP cells which were treated with S100A8/A9 (100 μg/ml) for 24 h (L). S100A8/A9 treatment induces typical morphology of mitochondrial fission inhibition (EM magnification: 8.5×10^3). (M) S100A8/A9 induced XIAP cleavage in SHEP cells. Western blot analysis of cell lysates from SHEP cells treated with 100 μg/ml S100A8/A9 for 0, 12, and 24 h, employing anti-XIAP. The 25-kD protein represents the degraded form. GAPDH was included as loading control.

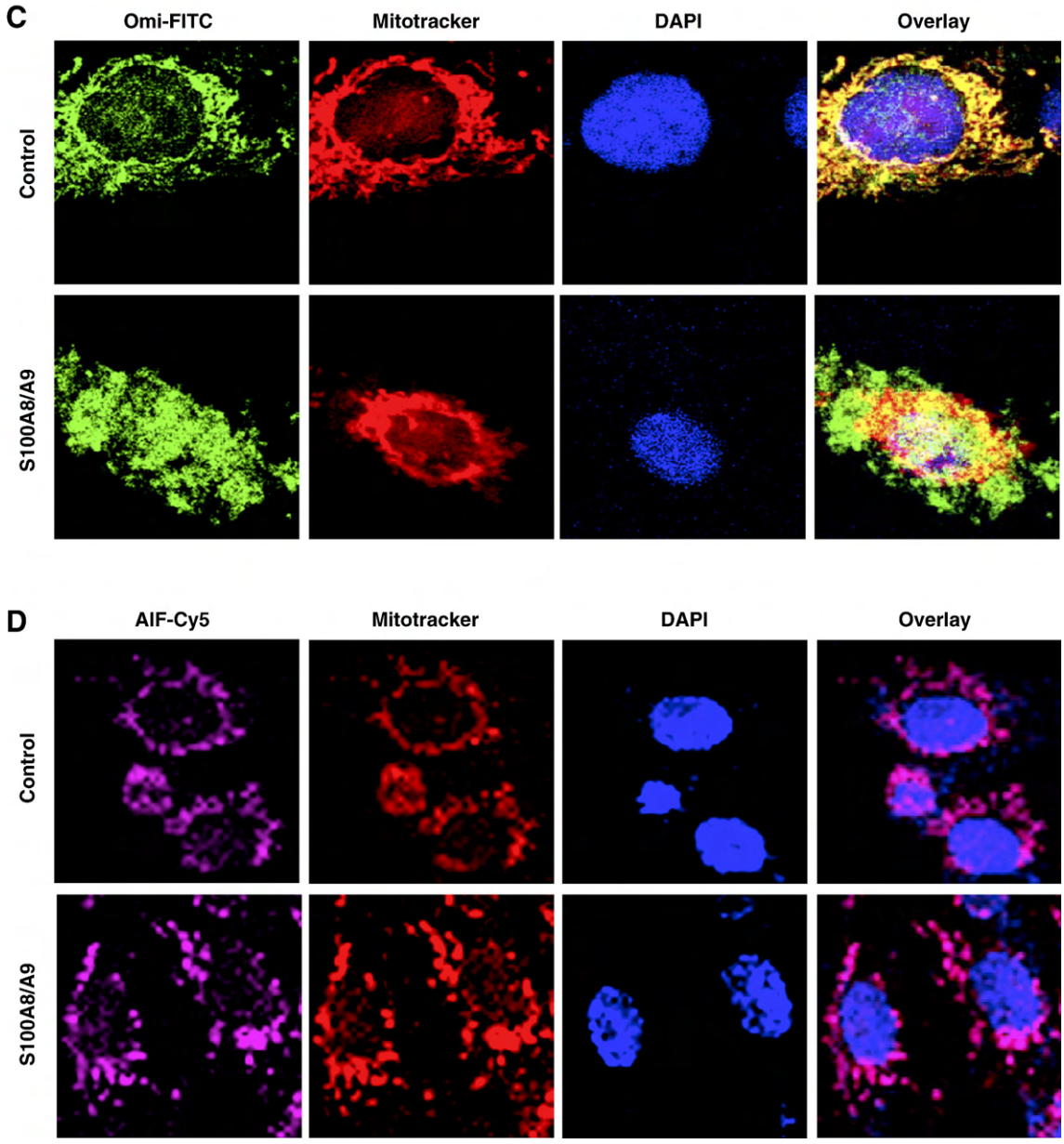

Fig. 4 (*continued*).

S100A8/A9 for 12 h and the subcellular location of Bax was investigated by confocal imaging and activation of Bak by immunoblotting. Treatment with S100A8/A9 did not result in translocation of Bax to the mitochondria (Fig. 4F, S100A8/A9 panel), but Bak homo-dimerization was detected by immunoblotting under non-denaturing and non-reducing conditions (Fig. 4G).

It has recently been reported that inhibiting one of the mitochondrial fission machinery proteins, Drp1, prevents the release of cytochrome *c* but not of Smac/DIABLO in Bax/Bak-dependent apoptosis [32]. Mitochondrial fission and fusion are normal and frequent events in healthy cells. The protein machinery that underlies mitochondrial fission has been well characterized and extensively reviewed [33]. In mammalian cells, the process requires at least three proteins, Drp1, hFis1 and MTP18 [34]. Drp1 is a large cytosolic GTPase that translocates to the mitochondria, where it couples GTP hydrolysis with scission of the mitochondrial tubule. Its receptor at the mitochondria surface is thought to be hFis1, which is anchored to the mitochondrial-inter-membrane facing the cytoplasm [34–36]. The treatment of SHEP cells with S100A8/A9 induced a significant decrease in Drp1 expression (Fig. 4J). This in turn induced the selective release of Smac/DIABLO and Omi/HtrA2 (Fig. 4B,C) without Bax translocation (Fig. 4F) but with Bak activation (Fig. 4G). The inhibition of mitochondrial fission machinery was confirmed using electron microscopy to study the ultrastructure of mitochondria in S100A8/A9 treated cells (Fig. 4L). The ultrastructure of mitochondria in S100A8/A9 treated cells showed typical morphology for the cells that their mitochondrial fission machinery was inhibited [32]. The

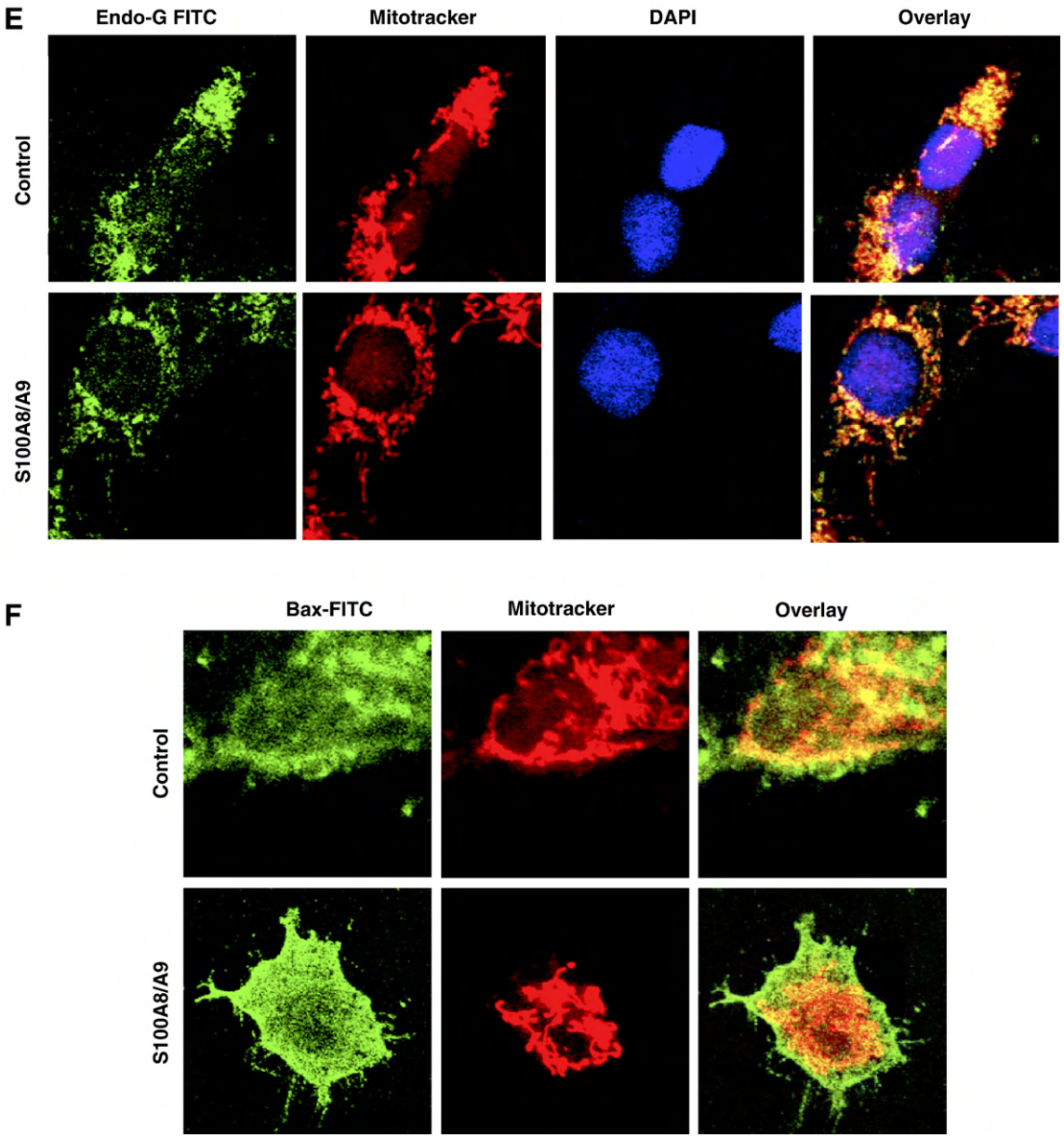

Fig. 4 (*continued*).

mitochondria showed partly disorganized structures, some of them actually inhibited at the stage of fission.

3.7. S100A8/A9 induces proteolytic cleavage of XIAP

XIAP is the most potent and best characterized member of mammalian IAP family [37,38]. Its caspase-inhibitory effect may be modified by mitochondria-derived negative regulators of apoptosis (Smac/DIABLO, Omi/HtrA2), which directly inhibit XIAP and are also able to promote XIAP phosphorylation and cleavage [38,39]. The treatment of SHEP cells with S100A8/A9 resulted in XIAP cleavage. As shown in Fig. 4M, the 25 kD fragment of XIAP could be detected 12 h after S100A8/A9 treatment, and the signal is pronounced at the 24 h time point, thus following the time course of the release of Smac/DIABLO in S100A8/A9 treated cells (Fig. 4B,C,H,I).

4. Discussion

S100A8/A9 is a unique molecule, capable of inducing cell death through multiple mechanisms that may play a critical role in cancer regression. S100A8/A9 positive cells, macrophages and polymorphonuclear leukocytes have been shown to accumulate along the invasive margin of a cancer [40]. Moreover, S100A8/A9 is released upon cellular activation [41] and induces apoptosis in malignant cells [1,42].

In order to elucidate the molecular mechanisms of S100A8/A9-induced cell death, we first compared the kinetics of apoptosis induced by S100A8/A9, and by the extracellular Zn-ion chelator DTPA. These experiments show that the apoptosis-inducing activity of S100A8/A9 is different from that of the membrane-impermeable zinc chelator DTPA. S100A8/A9 was not only more effective than DTPA (Supplementary Fig. 1A,B),

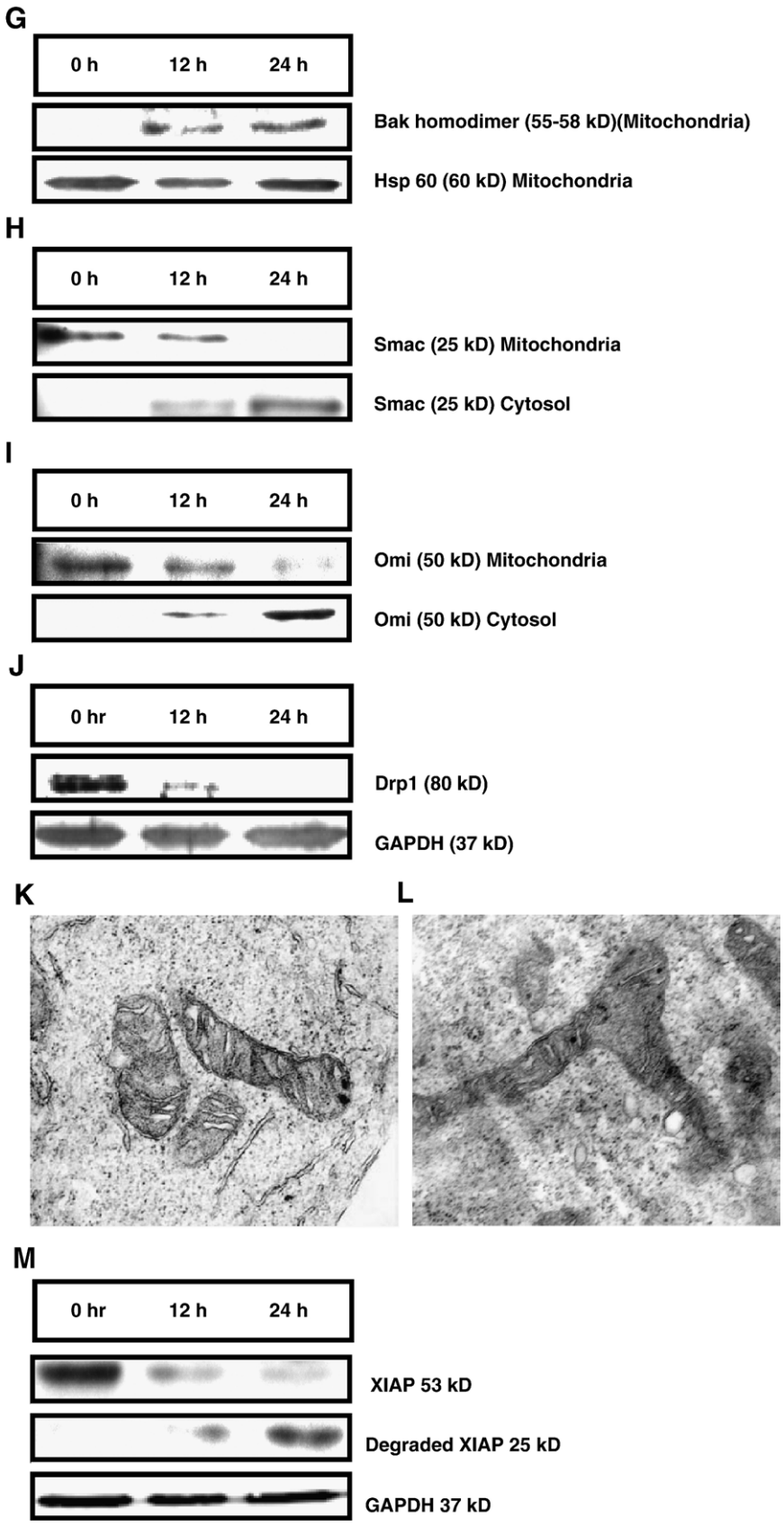

Fig. 4 (*continued*).

but furthermore, its apoptosis-inducing activity was not completely reversed by the addition of zinc ions (data not shown). Hence, S100A8/A9 appears to induce apoptosis by a mechanism that requires binding to target cells, and is distinct from the cell death caused by zinc depletion.

It has been proposed that RAGE serves as the receptor for the S100 family of proteins [7]. Thus, we performed detailed S100A8/A9 binding studies and analyzed RAGE expression by Western blot. The results showed that S100A8/A9 binds to all tested cell lines (Fig. 1A), and this interaction correlates with the presence of RAGE (Fig. 1B). Importantly, the experiments involving the inhibition of RAGE expression by specific siRNA, provided strong evidence that RAGE is a receptor for S100A8/A9 (Fig. 1C,D). However, these experiments also demonstrated that RAGE ligation is not involved in the induction of apoptosis by S100A8/A9 (Fig. 1E). This finding was further supported by experiments using a RAGE blocking antibody (Fig. 1F–H). Thus, a second, as yet unidentified receptor might mediate the apoptosis-inducing activity of S100A8/A9. Our results are consistent with reports of other putative cell surface-binding sites for S100A8/A9, including heparan sulfate proteoglycan [43], carboxylated glycans [44], and FAT/CD36 [45]. Interestingly, S100A8/A9 at low micromolar concentrations has growth-promoting activity and such activity relies on RAGE ligation and MAP-kinase dependent pathway [46]. This bimodal characteristic of S100A8/A9 is similar to another member of the S100 Ca-binding protein family, namely S100B. S100B, at concentrations ~100 nM induces apoptosis in myoblasts in a RAGE-independent manner [47]. S100B-triggered apoptosis was associated with ROS production and inhibition of the pro-survival ERK1/2-kinases. Other reports demonstrate that S100B behaves either as trophic or toxic factor, depending on concentration (reviewed by Donato [48]).

It is unlikely that S100A8/A9 triggers cell death via TNF-receptor-family death receptor. Death signaling via the TNF-death receptor family molecules typically involves the FADD adaptor protein [49]. FADD binds (directly or through another adaptor protein, TRADD) to the receptor via its interaction domain, DD, and to pro-caspase-8 through DED interactions to form a complex called DISC. Recruitment of caspase-8 through FADD leads to auto-cleavage and activation of the caspase [50]. We analyzed S100A8/A9 toxicity in Jurkat and BJAB cells, and their derivatives over-expressing a dominant-negative FADD-DN (Fig. 2A,B). These FADD-DN-expressing cells are protected from apoptosis if treated with anti-CD95 (Fig. 2C). However, the FADD-DN over-expressing cells did not differ from the corresponding wild type cells in their sensitivity toward S100A8/A9, both with respect to time course or effective dose. This finding is in accord with our previous report showing that S100A8/A9 did not induce caspase-8 activation [1].

It has been previously reported that treatment of HT29/249 and SW742 cells with S100A8/A9 increases the intracellular level of ROS, and antioxidants reversed the apoptosis-inducing activity of S100A8/A9 [1,42]. This prompted us to investigate the mitochondrial pathway in S100A8/A9-induced cell death using cellular models in which Bcl2 was over-expressed. Bcl2 family members promote or repress mitochondria-driven, and some other forms of programmed cell death. One function of the family is to influence the on/off state of the Mitochondrial Permeability Transition Pore (MPTP) [51]. For example, over-expression of Bcl2 reduces apoptosis in some models of neuronal ischemia [52]. Correspondingly, both Jurkat and MCF7 cells over-expressing Bcl2 were significantly more resistant to S100A8/A9-induced cell death ($P<0.05$) than their wild type counterparts (Fig. 3A,B). Further evidence for the involvement of the mitochondrial pathway in S100A8/A9-induced cell death was provided by our study of mitochondrial membrane potential (Ψ_m). S100A8/A9 caused a rapid drop in Ψ_m in MCF7 cells. However, MCF7 cells over-expressing Bcl2 were markedly protected from S100A8/A9-caused decrease in Ψ_m (Fig. 3C).

Treatment with S100A8/A9 caused the decrease in expression of Bcl2 and Bcl-X_L (Fig. 3D). It is still unclear exactly how the Bcl2 family proteins regulate apoptosis. Different models of regulation have been proposed in the literature. According to one model, the pro-apoptotic Bax and Bak are maintained in an inactive conformation through direct interactions with one or two different anti-apoptotic Bcl2 proteins. In response to an apoptotic stimulus, BH3-only proteins bind to and neutralize the anti-apoptotic Bcl2 proteins, thereby releasing Bax and Bak [25]. Over-expression of Bcl2 or Bcl-X_L has been reported to prevent Bax translocation and activation [53,54]. Furthermore, it has been reported that certain BH3-only proteins display selective interaction with specific anti-apoptotic Bcl2 family members. For instance, it has been reported that Bad interacts with Bcl2 and Bcl-X_L, but not with Mcl-1, whereas Noxa binds to Mcl-1, but not to Bcl2 and Bcl-X_L [25]. According to an alternative model, certain BH3-only proteins can interact with the pro-apoptotic proteins and trigger apoptosis by binding directly to Bax and Bak [25]. Finally, recent data suggest that anti-apoptotic Bcl2 family members sequester BH3-only proteins, preventing the activation of pro-apoptotic Bax and Bak. Eventually, the increasing number of activated BH3-only protein will overpower the anti-apoptotic Bcl2 proteins' inhibitory action, thereby triggering the death by direct activation of Bax/Bak, or possibly, activation of some other unknown factor in the cytosol or mitochondria required for Bax/Bak activation [25]. In addition it has been showed that mitochondrial depolarization could be prevented by over-expression of Bcl2 [25]. Our data indicate that high levels of Bcl2 expression partially protected from S100A8/A9-triggered $\Delta\Psi_m$ (Fig. 3C).

The release of cytochrome *c* is usually associated with Smac/DIABLO and Omi/HtrA2 in the apoptotic process after treatment with apoptosis inducers and other forms of cell stress [55–57]. However, in our study we failed to detect cytochrome *c* release, while Smac/DIABLO and Omi/HtrA2 were translocated to cytosol in S100A8/A9-treated cells (Fig. 4A–C,H,I). These observations are surprising because several papers have reported that the mitochondrial-inter-membrane proteins, cytochrome *c*, Smac/DIABLO and Omi/HtrA2 are released together with the same or similar kinetic pattern [57–59]. These proteins are mainly soluble in the inter membrane space. However, AIF is anchored to the inner membrane [60] and endonuclease G is likely mainly localized in the matrix [61], which would explain

the lack of AIF and endonuclease G in S100A8/A9-induced cell death as well as in other models.

Recently, a new model has emerged based on the discovery that cytochrome *c* is differentially released from other mitochondrial-inter-membrane proteins induced by Bax/Bak-dependent apoptosis in Drp1-depleted cells [32]. We showed that S100A8/A9-induced cell death was not Bax dependent, but Bak was activated and Drp1 expression was decreased. An explanation for the differential release of cytochrome *c* and Smac/DIABLO and Omi/HtrA2 in Drp1-depleted cells may be that the latter proteins are not as tightly bound to the mitochondria as cytochrome *c* [59]. Indeed, cytochrome *c* binds to protein partners (subunits of complexes III and IV) and phospholipids, in particular cardiolipin, through electrostatic interactions [62–64]. This implies that cytochrome *c* is more tightly bound to its interaction partners in Drp1-depleted cells than in control cells. Therefore our findings correlated and confirmed the recent findings on selective release of Smac/DIABLO and Omi/HtrA2 in the cells which mitochondrial fission machinery has been inhibited.

Mammalian Smac/DIABLO and Omi/HtrA2 have the ability to bind and antagonize the actions of IAPs. Cytosolic Omi/HtrA2 also contributes to both caspase-dependent and caspase-independent apoptosis [37]. Omi/HtrA2 interacts with cytosolic IAP proteins similar to Smac/DIABLO [56]. However, in contrast to Smac/DIABLO, HtrA2 also promotes the catalytic cleavage of IAPs leading to their irreversible inactivation and the progression of apoptosis [39]. Our finding that these proteins are selectively released from mitochondria in S100A8/A9-treated cells (Fig 4B,C) was confirmed by XIAP degradation to a 25-kD fragment (Fig. 4M).

In conclusion, the present study demonstrates that S100A8/A9 exerts cytotoxic activity in a broad range of cell lines. RAGE ligation is not involved in the death signaling activity of this protein but a second cell surface-binding site mediates the induction of apoptosis. S100A8/A9 decreases Ψ_m and causes Bak activation as well as decreased expression of Bcl2 and Bcl-X_L. In addition, S100A8/A9-induced cell death decreases Drp1 expression and provokes the selective translocation of Smac/DIABLO and Omi/HtrA2 from mitochondria to cytoplasm and subsequent XIAP degradation. In this study, we also report that inhibiting Drp1-mediated mitochondrial fission does not prevent Bak-mediated cell death, although it prevents cytochrome *c* release. Our results are in agreement with other time course study demonstrating that knock down of Drp1 does not inhibit apoptosis [32]. Hence, by tracing S100A8/A9 activity in cell death, this study provides an important insight into the molecular mechanism of the S100A8/A9 cell death pathway. It also provides an avenue for a better understanding of how S100A8/A9 released from activated phagocytes might be involved in the response of the innate immune system against tumors.

Acknowledgements

S.G. thankfully acknowledges fellowships form MHRC and CCMF. C.K. acknowledges the support through "Interdisziplinäres Zentrum für Klinische Forschung" (IZKF-project Ker3/086/04; to C.K.), "Deutsche Forschungsgemeinschaft" (DFG-projects KE 820/4-1 and KE 820/2-2; both to C.K.). W.J.C. has been supported through the US National Institutes of Health (RO1 GM62112). M.E. and A.Z. are thankful for their fellowships form CCMF and MICH. M.L. thankfully acknowledges support through CFI-Canada Research Chair program, CCMF-, MHRC-, CIHR, and MICH-founded programs. We thank Michael R. Miller for production of recombinant S100A8/S100A9.

Appendix A. Supplementary data

Supplementary data associated with this article can be found, in the online version, at doi:10.1016/j.bbamcr.2007.10.015.

References

[1] S. Ghavami, C. Kerkhoff, M. Los, M. Hashemi, C. Sorg, F. Karami-Tehrani, Mechanism of apoptosis induced by S100A8/A9 in colon cancer cell lines: the role of ROS and the effect of metal ions, J. Leukoc. Biol. 76 (2004) 169–175.

[2] M.P. McNamara, J.H. Wiessner, C. Collins-Lech, B.L. Hahn, P.G. Sohnle, Neutrophil death as a defence mechanism against Candida albicans infections, Lancet 2 (1988) 1163–1165.

[3] M. Steinbakk, C.F. Naess-Andresen, E. Lingaas, I. Dale, P. Brandtzaeg, M.K. Fagerhol, Antimicrobial actions of calcium binding leucocyte L1 protein, calprotectin, Lancet 336 (1990) 763–765.

[4] C. Kerkhoff, M. Klempt, C. Sorg, Novel insights into structure and function of MRP8 (S100A8) and MRP14 (S100A9), Biochem. Biophys. Acta 1448 (1998) 200–211.

[5] W. Nacken, J. Roth, C. Sorg, C. Kerkhoff, S100A9/S100A8: myeloid representatives of the S100 protein family as prominent players in innate immunity, Microsc. Res. Tech. 60 (2003) 569–580.

[6] C. Kerkhoff, W. Nacken, M. Benedyk, M.C. Dagher, C. Sopalla, J. Doussiere, The arachidonic acid-binding protein S100A8/A9 promotes NADPH oxidase activation by interaction with p67phox and Rac-2, FASEB J. 19 (2005) 467–469.

[7] M.A. Hofmann, S. Drury, C. Fu, W. Qu, A. Taguchi, Y. Lu, C. Avila, N. Kambham, A. Bierhaus, P. Nawroth, M.F. Neurath, T. Slattery, D. Beach, J. McClary, M. Nagashima, J. Morser, D. Stern, A.M. Schmidt, RAGE mediates a novel proinflammatory axis: a central cell surface receptor for S100/calgranulin polypeptides, Cell 97 (1999) 889–901.

[8] A.M. Schmidt, S.D. Yan, S.F. Yan, D.M. Stern, The multiligand receptor RAGE as a progression factor amplifying immune and inflammatory responses, J. Clin. Invest. 108 (2001) 949–955.

[9] A. Goldin, J.A. Beckman, A.M. Schmidt, M.A. Creager, Advanced glycation end products: sparking the development of diabetic vascular injury, Circulation 114 (2006) 597–605.

[10] H.J. Huttunen, J. Kuja-Panula, G. Sorci, A.L. Agneletti, R. Donato, H. Rauvala, Coregulation of neurite outgrowth and cell survival by amphoterin and S100 proteins through receptor for advanced glycation end products (RAGE) activation, J. Biol. Chem. 275 (2000) 40096–40105.

[11] Y. Nakatani, M. Yamazaki, W.J. Chazin, S. Yui, Regulation of S100A8/A9 (calprotectin) binding to tumor cells by zinc ion and its implication for apoptosis-inducing activity, Mediators Inflamm. 2005 (2005) 280–292.

[12] S. Yui, Y. Nakatani, M.J. Hunter, W.J. Chazin, M. Yamazaki, Implication of extracellular zinc exclusion by recombinant human calprotectin (MRP8 and MRP14) from target cells in its apoptosis-inducing activity, Mediators Inflamm. 11 (2002) 165–172.

[13] C. Kerkhoff, M. Klempt, V. Kaever, C. Sorg, The two calcium-binding proteins, S100A8 and S100A9, are involved in the metabolism of arachidonic acid in human neutrophils, J. Biol. Chem. 274 (1999) 32672–32679.

[14] M.J. Hunter, W.J. Chazin, High level expression and dimer characterization of the S100 EF-hand proteins, migration inhibitory factor-related proteins 8 and 14, J. Biol. Chem. 273 (1998) 12427–12435.

[15] S. Ghavami, K. Barczyk, S. Maddika, T. Vogl, L. Steinmüller, H. Pour-Jafari, J.A. Evans, M. Los, Monitoring of programmed cell death in vivo and in vitro, — new and old methods of cancer therapy assessment, in: M. Los, S.B. Gibson (Eds.), Apoptotic Pathways as Target for Novel Therapies in Cancer and Other Diseases, Springer Academic Press, New York, 2005, pp. 323–341.
[16] M. Hashemi, S. Ghavami, M. Eshraghi, E.P. Booy, M. Los, Cytotoxic effects of intra- and extracellular zinc chelation on human breast cancer cells, Eur. J. Pharm. 557 (2007) 9–19.
[17] S. Maddika, E.P. Booy, D. Johar, S.B. Gibson, S. Ghavami, M. Los, Cancer-specific toxicity of apoptin is independent of death receptors but involves the loss of mitochondrial membrane potential and the release of mitochondrial cell-death mediators by a Nur77-dependent pathway, J. Cell Sci. 118 (2005) 4485–4493.
[18] T. Koike, K. Kondo, T. Makita, K. Kajiyama, T. Yoshida, M. Morikawa, Intracellular localization of migration inhibitory factor-related protein (MRP) and detection of cell surface MRP binding sites on human leukemia cell lines, J. Biochem. (Tokyo) 123 (1998) 1079–1087.
[19] G.E. Weitsman, A. Ravid, U.A. Liberman, R. Koren, Vitamin D enhances caspase-dependent and independent TNF-induced breast cancer cell death: the role of reactive oxygen species, Ann. N.Y. Acad. Sci. 1010 (2003) 437–440.
[20] S. Maddika, G.H. Bay, T.J. Kroczak, S.R. Ande, S. Maddika, E. Wiechec, S.B. Gibson, M. Los, Akt is transferred to the nucleus of cells treated with apoptin, and it participates in apoptin-induced cell death, Cell Prolif. 40 (2007) 835–848.
[21] C. Stroh, U. Cassens, A.K. Samraj, W. Sibrowski, K. Schulze-Osthoff, M. Los, The role of caspases in cryoinjury: caspase inhibition strongly improves the recovery of cryopreserved hematopoietic and other cells, Faseb J. 16 (2002) 1651–1653.
[22] M. Mikami, M. Yamazaki, S. Yui, Kinetical analysis of tumor cell death-inducing mechanism by polymorphonuclear leukocyte-derived calprotectin: involvement of protein synthesis and generation of reactive oxygen species in target cells, Microbiol. Immunol. 42 (1998) 211–221.
[23] D. Hockenbery, G. Nunez, C. Milliman, R.D. Schreiber, S.J. Korsmeyer, Bcl-2 is an inner mitochondrial membrane protein that blocks programmed cell death, Nature 348 (1990) 334–336.
[24] P.T. Daniel, K. Schulze-Osthoff, C. Belka, D. Guner, Guardians of cell death: the Bcl-2 family proteins, Essays Biochem. 39 (2003) 73–88.
[25] A.B. Gustafsson, R.A. Gottlieb, Bcl-2 family members and apoptosis, taken to heart, American journal of physiology 292 (2007) C45–C51.
[26] H. Ye, C. Cande, N.C. Stephanou, S. Jiang, S. Gurbuxani, N. Larochette, E. Daugas, C. Garrido, G. Kroemer, H. Wu, DNA binding is required for the apoptogenic action of apoptosis inducing factor, Nat. Struct. Biol. 9 (2002) 680–684.
[27] L.Y. Li, X. Luo, X. Wang, Endonuclease G is an apoptotic DNase when released from mitochondria, Nature 412 (2001) 95–99.
[28] N.N. Danial, S.J. Korsmeyer, Cell death: critical control points, Cell 116 (2004) 205–219.
[29] S. Cory, J.M. Adams, The Bcl2 family: regulators of the cellular life-or-death switch, Nat. Rev. Cancer 2 (2002) 647–656.
[30] K. Degenhardt, R. Sundararajan, T. Lindsten, C. Thompson, E. White, Bax and Bak independently promote cytochrome *C* release from mitochondria, J. Biol. Chem. 277 (2002) 14127–14134.
[31] M.G. Vander Heiden, C.B. Thompson, Bcl-2 proteins: regulators of apoptosis or of mitochondrial homeostasis? Nat. Cell Biol. 1 (1999) E209–E216.
[32] P.A. Parone, D.I. James, S. Da Cruz, Y. Mattenberger, O. Donze, F. Barja, J.C. Martinou, Inhibiting the mitochondrial fission machinery does not prevent Bax/Bak-dependent apoptosis, Mol. Cell Biol. 26 (2006) 7397–7408.
[33] D.A. Rube, A.M. van der Bliek, Mitochondrial morphology is dynamic and varied, Mol. Cell. Biochem. 256–257 (2004) 331–339.
[34] R.J. Youle, M. Karbowski, Mitochondrial fission in apoptosis, Nat. Rev. Mol. Cell Biol. 6 (2005) 657–663.
[35] Y. Yoon, E.W. Krueger, B.J. Oswald, M.A. McNiven, The mitochondrial protein hFis1 regulates mitochondrial fission in mammalian cells through an interaction with the dynamin-like protein DLP1, Mol. Cell Biol. 23 (2003) 5409–5420.
[36] T. Yu, R.J. Fox, L.S. Burwell, Y. Yoon, Regulation of mitochondrial fission and apoptosis by the mitochondrial outer membrane protein hFis1, J. Cell Sci. 118 (2005) 4141–4151.
[37] U. Cassens, G. Lewinski, A.K. Samraj, H. von Bernuth, H. Baust, K. Khazaie, M. Los, Viral modulation of cell death by inhibition of caspases, Arch. Immunol. Ther. Exp. 51 (2003) 19–27.
[38] H.G. Zhang, J. Wang, X. Yang, H.C. Hsu, J.D. Mountz, Regulation of apoptosis proteins in cancer cells by ubiquitin, Oncogene 23 (2004) 2009–2015.
[39] Y. Suzuki, Y. Imai, H. Nakayama, K. Takahashi, K. Takio, R. Takahashi, A serine protease, HtrA2, is released from the mitochondria and interacts with XIAP, inducing cell death, Molecular cell 8 (2001) 613–621.
[40] J. Stulik, J. Osterreicher, K. Koupilova, J. Knizek, A. Macela, J. Bures, P. Jandik, F. Langr, K. Dedic, P.R. Jungblut, The analysis of S100A9 and S100A8 expression in matched sets of macroscopically normal colon mucosa and colorectal carcinoma: the S100A9 and S100A8 positive cells underlie and invade tumor mass, Electrophoresis 20 (1999) 1047–1054.
[41] A. Rammes, J. Roth, M. Goebeler, M. Klempt, M. Hartmann, C. Sorg, Myeloid-related protein (MRP) 8 and MRP14, calcium-binding proteins of the S100 family, are secreted by activated monocytes via a novel, tubulin-dependent pathway, J. Biol. Chem. 272 (1997) 9496–9502.
[42] C. Kerkhoff, S. Ghavami, Induction of apoptotic cell death in tumor cells by S100A8/A9 released from inflammatory cells upon cellular activation, Current Medical Chemistry (AIAA) 4 (2005) 383–391.
[43] M.J. Robinson, P. Tessier, R. Poulsom, N. Hogg, The S100 family heterodimer, MRP-8/14, binds with high affinity to heparin and heparan sulfate glycosaminoglycans on endothelial cells, J. Biol. Chem. 277 (2002) 3658–3665.
[44] G. Srikrishna, K. Panneerselvam, V. Westphal, V. Abraham, A. Varki, H.H. Freeze, Two proteins modulating transendothelial migration of leukocytes recognize novel carboxylated glycans on endothelial cells, J. Immunol. 166 (2001) 4678–4688.
[45] C. Kerkhoff, C. Sorg, N.N. Tandon, W. Nacken, Interaction of S100A8/S100A9-arachidonic acid complexes with the scavenger receptor CD36 may facilitate fatty acid uptake by endothelial cells, Biochemistry 40 (2001) 241–248.
[46] S. Ghavami, I. Rashedi, B.M. Dattilo, M. Eshraghi, W.J. Chazin, M. Hashemi, S. Wesselborg, C. Kerkhoff, M. Los, S100A8/A9 at low concentration, promotes tumor cell growth via RAGE ligation and MAP-kinase dependent pathway, J. Leukoc. Biol. (2008) (provisionally accepted).
[47] G. Sorci, F. Riuzzi, A.L. Agneletti, C. Marchetti, R. Donato, S100B causes apoptosis in a myoblast cell line in a RAGE-independent manner, J. Cell Physiol. 199 (2004) 274–283.
[48] R. Donato, Intracellular and extracellular roles of S100 proteins, Microsc. Res. Tech. 60 (2003) 540–551.
[49] M. Los, S. Wesselborg, K. Schulze-Osthoff, The role of caspases in development, immunity, and apoptotic signal transduction: lessons from knockout mice, Immunity 10 (1999) 629–639.
[50] E.O. Gomez, C. Mendoza-Milla, M.J. Ibarra-Sanchez, J.L. Ventura-Gallegos, A. Zentella, Ceramide reproduces late appearance of oxidative stress during TNF-mediated cell death in L929 cells, Biochem. Biophys. Res. Commun. 228 (1996) 505–509.
[51] D.R. Green, G. Kroemer, The pathophysiology of mitochondrial cell death, Science 305 (2004) 626–629.
[52] A.J. Kowaltowski, R.G. Cosso, C.B. Campos, G. Fiskum, Effect of Bcl-2 overexpression on mitochondrial structure and function, J. Biol. Chem. 277 (2002) 42802–42807.
[53] D.M. Finucane, E. Bossy-Wetzel, N.J. Waterhouse, T.G. Cotter, D.R. Green, Bax-induced caspase activation and apoptosis via cytochrome *c* release from mitochondria is inhibitable by Bcl-xL, J. Biol. Chem. 274 (1999) 2225–2233.
[54] A. Van Laethem, S. Van Kelst, S. Lippens, W. Declercq, P. Vandenabeele, S. Janssens, J.R. Vandenheede, M. Garmyn, P. Agostinis, Activation of p38 MAPK is required for Bax translocation to mitochondria, cytochrome *c* release and apoptosis induced by UVB irradiation in human keratinocytes, Faseb J. 18 (2004) 1946–1948.
[55] C. Adrain, S.J. Martin, The mitochondrial apoptosome: a killer unleashed by the cytochrome seas, Trends Biochem. Sci. 26 (2001) 390–397.

[56] M. van Gurp, N. Festjens, G. van Loo, X. Saelens, P. Vandenabeele, Mitochondrial intermembrane proteins in cell death, Biochem. Biophys. Res. Commun. 304 (2003) 487–497.

[57] G. van Loo, M. van Gurp, B. Depuydt, S.M. Srinivasula, I. Rodriguez, E.S. Alnemri, K. Gevaert, J. Vandekerckhove, W. Declercq, P. Vandenabeele, The serine protease Omi/HtrA2 is released from mitochondria during apoptosis. Omi interacts with caspase-inhibitor XIAP and induces enhanced caspase activity, Cell Death Differ. 9 (2002) 20–26.

[58] C. Munoz-Pinedo, A. Guio-Carrion, J.C. Goldstein, P. Fitzgerald, D.D. Newmeyer, D.R. Green, Different mitochondrial intermembrane space proteins are released during apoptosis in a manner that is coordinately initiated but can vary in duration, Proc. Natl. Acad. Sci. U. S. A. 103 (2006) 11573–11578.

[59] R.T. Uren, G. Dewson, C. Bonzon, T. Lithgow, D.D. Newmeyer, R.M. Kluck, Mitochondrial release of pro-apoptotic proteins: electrostatic interactions can hold cytochrome *c* but not Smac/DIABLO to mitochondrial membranes, J. Biol. Chem. 280 (2005) 2266–2274.

[60] H. Otera, S. Ohsakaya, Z. Nagaura, N. Ishihara, K. Mihara, Export of mitochondrial AIF in response to proapoptotic stimuli depends on processing at the intermembrane space, Embo J. 24 (2005) 1375–1386.

[61] D. Arnoult, B. Gaume, M. Karbowski, J.C. Sharpe, F. Cecconi, R.J. Youle, Mitochondrial release of AIF and EndoG requires caspase activation downstream of Bax/Bak-mediated permeabilization, Embo J. 22 (2003) 4385–4399.

[62] S. Ferguson-Miller, D.L. Brautigan, E. Margoliash, Correlation of the kinetics of electron transfer activity of various eukaryotic cytochromes *c* with binding to mitochondrial cytochrome *c* oxidase, J. Biol. Chem. 251 (1976) 1104–1115.

[63] S.L. Iverson, S. Orrenius, The cardiolipins–cytochrome *c* interaction and the mitochondrial regulation of apoptosis, Arch. Biochem. Biophys. 423 (2004) 37–46.

[64] E. Mochan, P. Nicholls, Cytochrome *c* reactivity in its complexes with mammalian cytochrome *c* oxidase and yeast peroxidase, Biochim. Biophys. Acta 267 (1972) 309–319.